

Electronic Supporting Information (ESI)

Periodic Mesoporous Titania with Anatase and Bronze Phases - The New Generation Photocatalyst: Synthesis, Characterisation and Application in Environmental Remediation

Surya Kumar Vatti^{a†}, Sanjeev Gupta^{a†}, Rayappan Pavul Raj^a and Parasuraman Selvam^{a,b,c,d*}

*^aNational Centre For Catalysis Research and Department of Chemistry,
Indian Institute of Technology-Madras, Chennai 600036, India*

*^bSchool of Chemical Engineering and Analytical Science,
The University of Manchester, Manchester M13 9PL, United Kingdom*

*^cDepartment of Chemical and Process Engineering
University of Surrey, Guildford, Surrey GU2 7XH, United Kingdom*

*^dDepartment of Chemistry, Faculty of Advanced Science and Technology,
Kumamoto University, 2-39-1 Kurokami, Chuo-ku, Kumamoto 860-8555, Japan*

*Corresponding Author.

Tel.: +91 -44-2257-4235/4200

E-mail: selvam@iitm.ac.in

This PDF file includes:

ESI Calibration of HPLC, S1

ESI Calibration of UV-Vis spectra, S2

ESI Figures, S1-S7

ESI Table S1

S1. Calibration of HPLC for estimation of famotidine

HPLC was calibrated by preparing different concentrations (10 to 100 ppm) of famotidine (FAM) in distilled water. FAM exhibits two absorption peaks due to $\pi \rightarrow \pi^*$ and $n \rightarrow \pi^*$ transitions (Figure S4). The mobile phase employed was 7% methanol to 93% Mili-Q water with 0.2% formic acid. The eluent flow was 1 mL/min with oven temperature at 35°C and the wavelength of detection was 266 nm, and the FAM eludes at 10 min. The linear response of the detector for FAM peak area was observed at five different concentrations ranging from 10 to 100 ppm. The Calibration plot was linear in the study range with a correlation coefficient of 0.999, and the equation of regression analysis: $y = 32989x + 24618$ (see Figure S5).

S2. Calibration of UV-Vis spectra for estimation of 4-chlorophenol

UV-VIS spectra were calibrated by preparing different concentrations (5 to 40 ppm) of 4-chlorophenol (4-CP) in distilled water. 4-CP exhibits two absorption peaks due to $\pi \rightarrow \pi^*$ and $n \rightarrow \pi^*$ transitions (see Figure S6). The absorbance at $\lambda_{\max} = 225$ nm was chosen for the calibration plot and the concentration of samples generated during degradation experiments was calculated from linear plot of the calibration plot with a correlation coefficient of 0.997, and the equation of the regression analysis: $y = 0.047x + 0.116$ (see Figure S7).

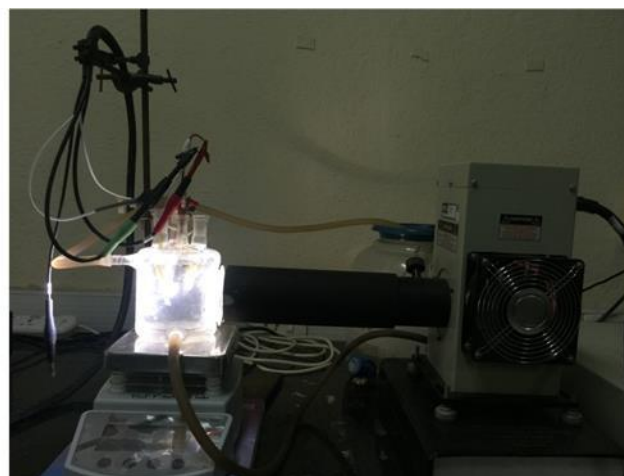
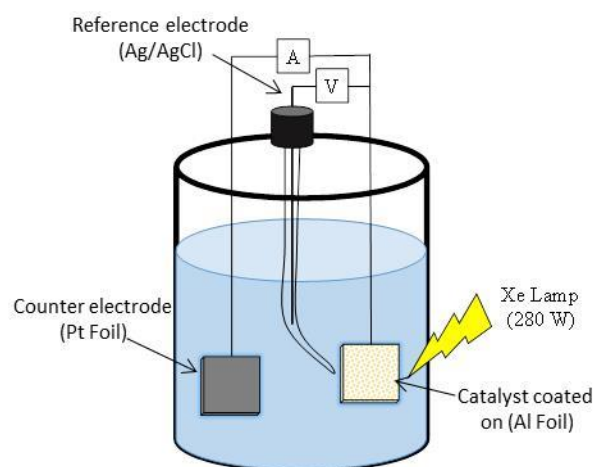


Figure S1. Photo-electrochemical reactor set-up: (a) Schematic; (b) Experimental system.

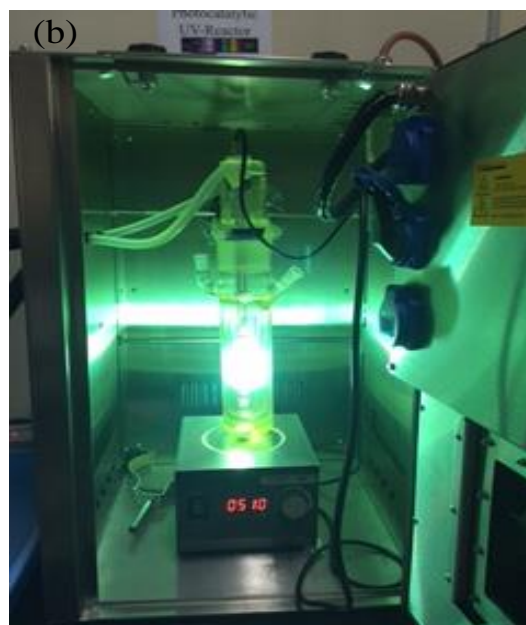
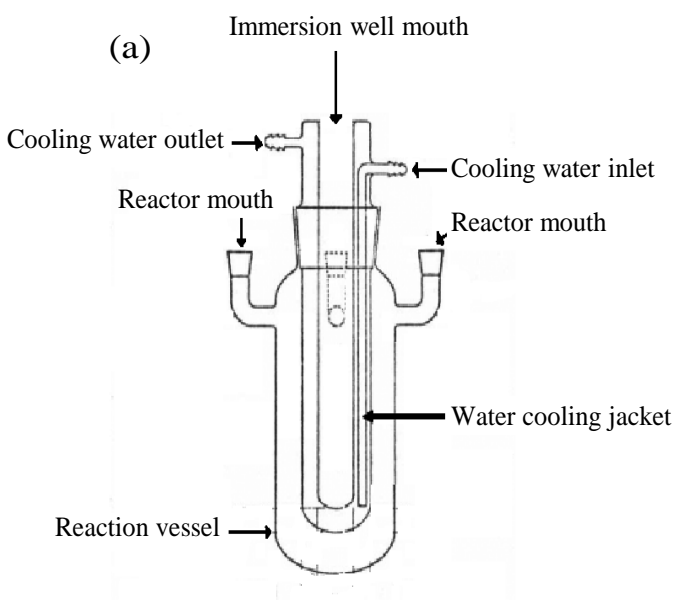


Figure S2. Photocatalytic reactor set-up: (a) Schematic; (b) Working reactor system in a UV-protective cabinet.

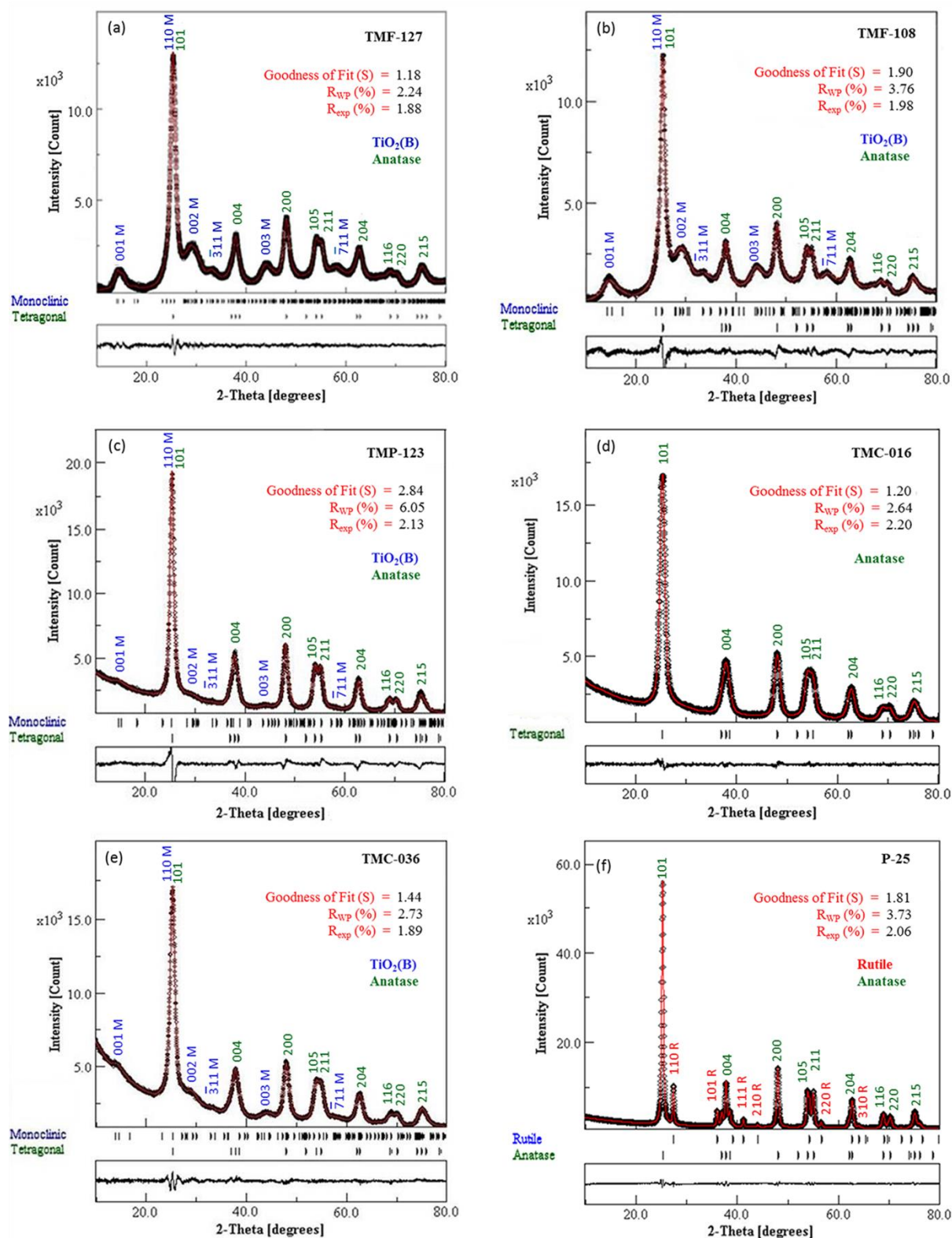


Figure S3. The Rietveld refined experimental, calculated and difference XRD patterns of: (a) TMF-127; (b) TMF-108; (c) TMP-123; (d) TMC-016; (e) TMC-036; (f) P-25. The vertical lines indicate the Bragg positions of the different phases.

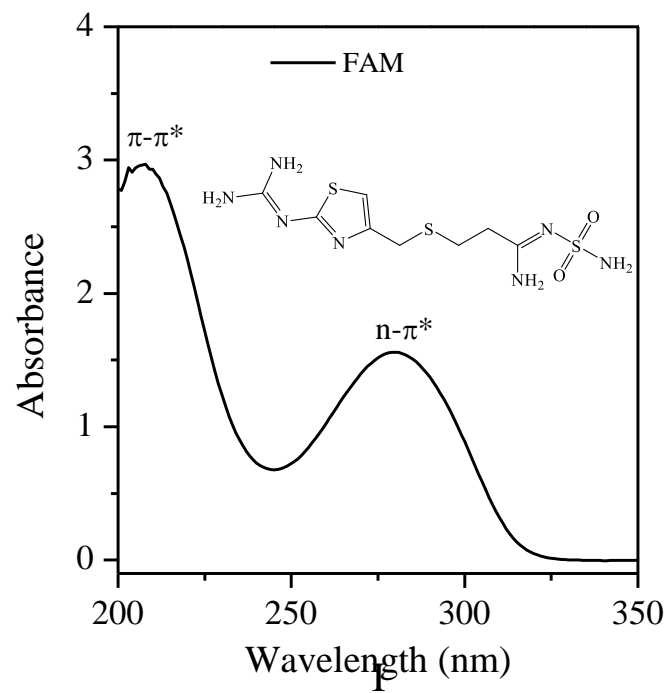


Figure S4 . UV-VIS spectrum of famotidine.

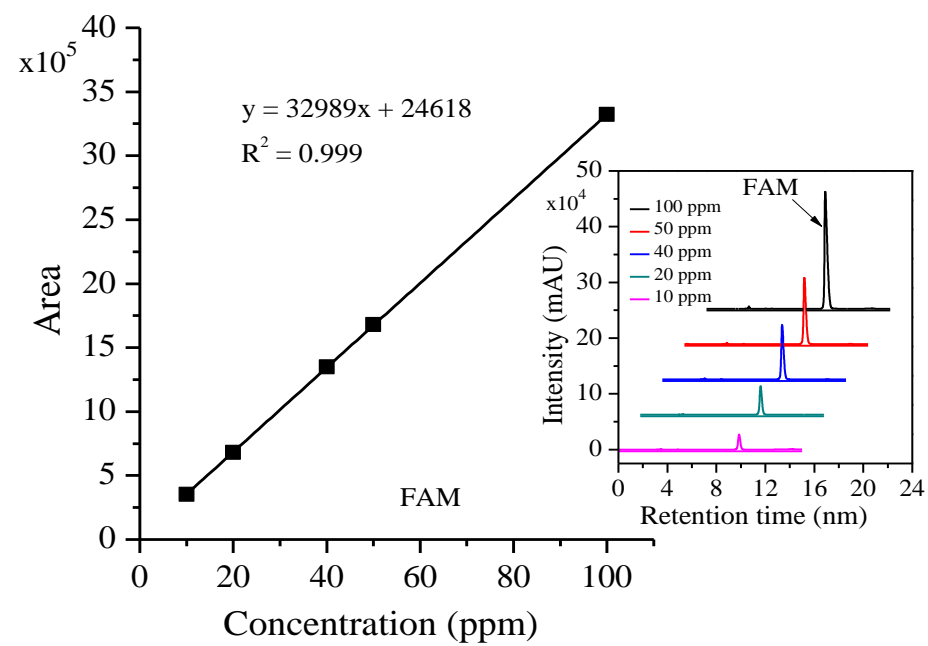


Figure S5. HPLC profile and calibration plot of FAM for quantitative analysis.

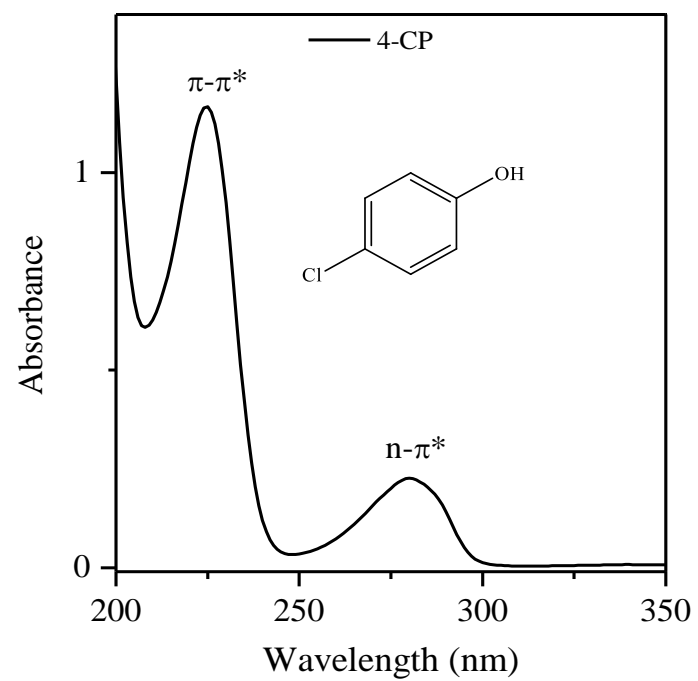


Figure S6 . UV-VIS spectrum of 4-chlorophenol.

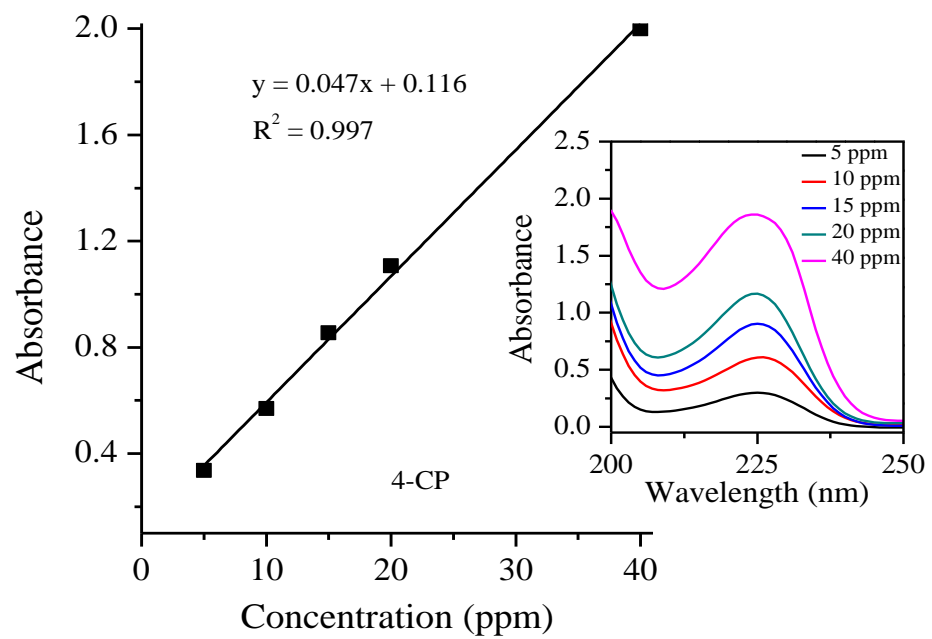


Figure S7. UV spectra and calibration plot of 4-CP for quantitative analysis.

Table S1. Observed room temperature Raman spectral frequencies (cm^{-1}) and their assignment for various titania samples.¹⁻⁵

Material	TiO ₂ - Anatase [†]						TiO ₂ - Bronze							TiO ₂ - Rutile [§]	
	$E_g(1)$	$E_g(2)$	$B_{1g}(1)$	$A_{1g}+B_{1g}$	$E_g(3)$	$B_{1g}(1)^{\ddagger}$	$B_g(1)$	$A_g(1)$	$B_g(2)$	$B_g(3)$	$A_g(2)$	$A_g(3)$	$A_g(4)$	E_g	A_{1g}
TMF-127	146	198	398	517	638	796	126	145	199	248	365	475	665	--	--
TMF-108	144	196	397	517	637	796	124	143	197	247	362	474	665	--	--
TMP-123	145	196	397	517	639	793	124	144	198	247	365	474	663	--	--
TMC-016	145	198	396	516	639	792	--	--	--	--	--	--	--	--	--
TMC-036	145	198	398	516	638	798	124	143	199	248	366	473	663	--	--
P-25	147	197	397	517	637	796	--	--	--	--	--	--	--	447	605

[†]At low temperature (73 K), the Raman band occurring at 516 cm^{-1} (298 K) is split into two bands centered at 513 and 519 cm^{-1} , and are assigned to A_{1g} and $B_{1g(2)}$ modes, respectively.

[‡]First overtone mode of $B_{1g}(1)$ mode.

[§]At room temperature, the rutile structure exhibits four first order Raman active modes,² i.e., B_{1g} (144 cm^{-1}), E_g (448 cm^{-1}), A_{1g} (612 cm^{-1}) and B_{2g} (827 cm^{-1}). Since the scattering intensity of the B_{2g} mode is very weak while the B_{1g} mode is relatively weak and overlaps to that of the E_g (147 cm^{-1}) strong mode in anatase, they are not visible in the recorded spectra.

References

1. T. Ohsaka, F. Izumi and Y. Fujiki, *J. Raman Spectrosc.*, 1978, **7**, 321.
2. U. Balachandran and N.G. Error, *J. Solid State Chem.*, 1982, **42**, 276.
3. T.D. Robert, L.D. Laude, V.M. Geskin, R. Lazzaroni, and R. Gouttebaron, *R. Thin Sol. Films*, 2003, **440**, 268.
4. M.B. Yahia, F. Lemoigno, T. Beuvier, J.-S. Filhol, M. Richard-Plouet, L. Brohan and M.-L. Doublet, *J. Chem. Phys.*, 2009, **130**, 204501.
5. T. Beuvier, M. Richard-Plouet and L. Brohan, *J. Phys. Chem. C*, 2009, **113**, 13703.